Aging Impact on Relative Permittivity, Thermal Properties, and Lightning Impulse Voltage Performance of Natural Ester Oil Filled With Semiconducting Nanoparticles

Konstantinos N. Koutras, Georgios D. Peppas, *Senior Member, IEEE*, Sokratis N. Tegopoulos, Apostolos Kyritsis, Andreas G. Yiotis, Thomas E. Tsovilis, *Senior Member, IEEE*, Ioannis F. Gonos, *Senior Member, IEEE*, and Eleftheria C. Pyrgioti, *Member, IEEE*

***Abstract*— This study is focused on exploring the change in the dielectric and cooling efficiency of vegetable oil following the integration of semiconducting SiC and TiO_2 nanoparticles (NPs) in two different weight percentages by comparing the corresponding behavior of nanofluids (NFs) at the time of their synthesis and after one month of aging. The thermal response has been evaluated by means of diffusivity and conductivity, while dielectric properties are measured with nondestructive tests (relative permittivity and dissipation factor) and destructive ones in terms of lightning impulse withstand voltage. The results of the latter property measurements are also compared to numerical model findings. The analysis of results proves that the properties under study are worsened with increase in NPs' concentration, probably attributing it to quicker agglomeration, as it is also confirmed by the simulation results.**

***Index Terms*— Aging, lightning impulse breakdown voltage (LI BDV), nanofluid (NF), relative permittivity, thermal conductivity.**

Manuscript received 18 December 2022; revised 10 March 2023 and 25 May 2023; accepted 9 June 2023. Date of publication 13 June 2023; date of current version 21 August 2023. *(Corresponding author: Konstantinos N. Koutras.)*

Konstantinos N. Koutras and Eleftheria C. Pyrgioti are with the Department of Electrical and Computer Engineering, University of Patras, 26504 Patras, Greece (e-mail: k.koutras@ece.upatras.gr; e.pyrgioti@ece.upatras.gr).

Georgios D. Peppas is with Raycap S.A., 66100 Drama, Greece (e-mail: peppas@ece.upatras.gr).

Sokratis N. Tegopoulos and Apostolos Kyritsis are with the School of Applied Mathematics and Physical Sciences, National Technical University of Athens, 15780 Athens, Greece (e-mail: stegopoulos@mail.ntua.gr; akyrits@central.ntua.gr).

Andreas G. Yiotis is with the School of Mineral Resources Engineering, Technical University of Crete, 73100 Chania, Greece (e-mail: agiotis@tuc.gr).

Thomas E. Tsovilis is with the School of Electrical and Computer Engineering, Aristotle University of Thessaloniki, 54124 Thessaloniki, Greece (e-mail: tsovilis@auth.gr).

Ioannis F. Gonos is with the School of Electrical and Computer Engineering, National Technical University of Athens, 15780 Athens, Greece (e-mail: igonos@cs.ntua.gr).

Color versions of one or more figures in this article are available at https://doi.org/10.1109/TDEI.2023.3285524.

Digital Object Identifier 10.1109/TDEI.2023.3285524

I. Introduction

THE effect of different nanoparticles (NPs) on the thermal and dielectric properties of dielectric liquids, which are largely used in power transformers as dielectric materials and coolants, has drawn a lot of interest in the past few years [1], [2], [3], [4], [5], [6], [7], [8], [9], [10], [11], [12], [13], [14], [15], [16], [17], [18]. Focusing on both dielectric and thermal properties, it is critical for the design and development criteria of immersed power transformers. Although the reported findings are frequently contradictory, the method of adding NPs to conventional oil volumes, the formation of a new dielectric liquid that is called nanofluid (NF), has revealed promising results in improving a range of characteristics [1], [2], [3], [4], [5], [6]. Mineral oils (MOs), despite being used almost exclusively as liquid insulation in high-voltage (HV) applications up to this point, have serious drawbacks, as they are very flammable, highly toxic, and have short lifetime, facts which turn the attention to environment conscious natural ester oils (NEOs) and synthetic ester oils (SEOs) on a global scale [6], [7], [8], [9], [10]. However, ester oils have their disadvantages as well, because there are many studies reporting lower breakdown voltage and higher dissipation factor with respect to MOs [17], [19]. The research on the addition of NPs in natural ester aims to find a proper insulating NF with a particular type of NP in a suitable concentration level, which is characterized by improved dielectric and physicochemical properties to propose it as a proper replacement of the MO.

In this direction, Khaled and Beroual [1] noticed that incorporating Fe_3O_4 NPs at 0.4 g/L ratio in a NEO can lead to expected ac breakdown voltage (ac BDV) enhancement by 48%. According to Fasehullah et al. [9], the introduction of CdS NPs in SEO can result in an about 35% improvement of the ac BDV at a 0.3 g/L loading. Furthermore, Koutras et al. [18] and Khelifa et al. [10] investigated partial discharge (PD) activity in NEO filled with SiC NPs and SEO doped with fullerene NPs, respectively. Koutras et al. [18]

found that the integration of SiC NPs at 0.004% w/w can improve the PD inception voltage (PDIV) by around 40%, while adding fullerene NPs can considerably delay the PDIV [10].

On account of lightning impulse breakdown voltage (LI BDV) performance under positive polarity, Sima et al. [11] examined the impact of surface-modified conductive Fe_3O_4, semiconductive TiO_2, and insulative Al_2O_3 NPs on MO at the same concentrations. The results proved that the NF containing the conductive NPs resulted in the highest LI BDV increment. The authors explained those results by introducing the ability of colloids to trap fast-moving electrons by forming a potential well around their surface, where the streamer's high-energy electrons could be captured. The value of this potential well is higher, the higher the contrast of conductivity (if the NP is conductive) or dielectric constant (for semiconductive or insulative NP) between NP and host liquid. For negative LI BDV efficiency, Beroual and Khaled [5] referred that a 16.8% improvement can be achieved by integrating a 0.05 g/L amount of Al_2O_3 NPs in NEO.

Despite the variety of experimental investigation of dielectric properties of NFs based on environmentally friendly oils, there are limited works studying the relative permittivity and thermal efficiency in terms of diffusivity and thermal conductivity, although the thermal performance of NF is equally important for its choice as a potential candidate for MO replacement in power transformers [8], [12], [13]. Besides, it is well known that conventional colloidal suspensions tend to agglomerate with time resulting in sedimentation; thus, a change occurs in their active concentration inside the liquid volume [7], [13], [14]; nevertheless, thermolytic root (thermal decomposition) coating methods of nanocrystals can surpass the latter agglomerates successfully [19]. However, the evolution of dielectric and thermal properties over aging time has yet to be explored extensively. The influence of bentonite on thermally aged vegetable oil-based NF incorporating TiO_2 NPs was analyzed by Amalanathan et al. [15]. They claimed that the dissipation factor of NFs was higher when compared to the matrix during thermal aging. It has also been reported that the addition of a variety of NPs leads to an increase in dissipation factor with respect to the pure oil's during aging [16]. The experiments at the whole of these works, however, only happened at room temperature.

In this study, the thermal properties of four natural ester-based NFs with weight percentage ratios of TiO_2 and SiC NPs of 0.004% and 0.008%, respectively, are determined in terms of thermal conductivity and thermal diffusivity over the temperature range of 25 °C–90 °C. Additionally, relative permittivity and dielectric dissipation factor (tand) of the NF and matrix samples are evaluated and processed at a frequency range from 1 to 10^6 Hz at room and elevated temperatures. All of the experiments take place shortly after the synthesis of NFs and are repeated with the same protocol after they are one-month aged. This study is focused on the influence of metal carbide NPs (like SiC) affecting the dielectric and thermal properties of dielectric liquids, which have not been extensively investigated in the literature, such as the ones of TiO_2 and other metal oxide NPs (i.e., Fe_3O_4, Fe_2O_3, and Al_2O_3) [1], [5], [19]. As described in [18], the stability of the same dispersions of TiO_2 and SiC NPs had been examined *in situ* in room and high temperatures for a range of weeks. Their performance at 90 °C is also evaluated, apart from the ambient, since it is of major interest for high load conditions of power transformers. The results of this study can assist in leading to valuable findings on the effect of colloidal stability on the evolution of the dielectric and thermal performance in the field of NFs.

Apart from the aforementioned properties, the samples containing SiC NPs are also subjected to positive lightning impulse voltage (LIV) after their synthesis and the outcomes are contrasted to the ones of a numerical model developed in COSMOL Multiphysics graphical environment [17].

II. Materials and Methods

A. Justification of the Materials Used

The base for the synthesis of NFs is Cargill's NEO FR3. The selected TiO_2 (21 nm average diameter) and SiC (50 nm average diameter) NPs have been obtained commercially from Sigma Aldrich and NanoAmor, respectively, and characterized from a spherical shape. NPs with semiconducting nature were selected due to the absence of literature and prior art on SiC NF, while there is extensive one on the impact of conductive NPs [1], [5], [19]; with respect to the dielectric NPs, like SiO_2 [12], they are not so effective because their dielectric constant is similar to the matrix oil's [11].

The analytical descriptions of the aforementioned materials' properties can be found in earlier research [8], [13], [17]. The DRS method is utilized to determine the relative permittivity ε_r of matrix and NPs in complex form, as indicated from the following equation [13], [17]:

$$\varepsilon_r = \varepsilon_r' - j\varepsilon_r'' \tag{1}$$

where ε_r' is called dielectric constant reflecting the stored energy in the dielectric and ε_r'' stands for the imaginary part, which expresses the dielectric losses induced by polarization and leakage current. In brief, NPs in white nanopowder are put into a test cell with 20-mm-diameter golden spherical electrodes, which are then introduced into the Novocontrol BDS1200 cell to conduct the dielectric relaxation measurements. On the other hand, the base oil sample is placed in a cylindrical sample holder capacitor also supplied by Novocontrol (BDS1307 cylindrical liquid cell). All capacitor samples are subjected to the same ac voltage applied by a Novocontrol Alpha analyzer with both parts of relative permittivity recorded at a frequency range from 1 Hz to 1 MHz.

Following the measurement of relative permittivity, the tand is calculated from the following equation:

$$\text{tand} = \frac{\varepsilon_r''}{\varepsilon_r'}. \tag{2}$$

An earlier study included the variation of the frequency-dependent relative permittivity for the NPs in question [17]. From those results, it was evident that the dielectric constant of SiC NPs, probably due to their carbon-rich surface [18], is higher with respect to the corresponding one of the TiO_2 at the whole understudy spectrum.

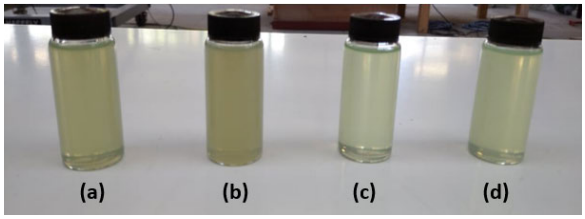

Fig. 1. NF samples after their homogenization.(a) sNF1 (b) sNF2 (c) tNF1 (d) tNF2.

B. Synthesis of NF Samples

The preparation of the understudy NF samples includes two phases (two-step method). In this method, NPs are usually commercially accessible and produced by applying physical, chemical, and mechanical practices for the first phase. The grown dry NPs are usually uniformly dispersed in base liquid volumes using ultrasonic bath followed by magnetic stirring for the second phase. For the understudied NFs, ultrasonication was adopted.

Initially, the integration of the dry NPs in the matrix vegetable oil volume takes place at the selected concentration levels, namely, 0.0004% and 0.008% w/w, synthesizing two NEO-based TiO_2 and two NEO-based SiC NFs. It is worth mentioning that no surfactants have been used for the surface modification of the NPs, as long the aim of our study is to provide a comparison of their influence without any modification. Apart from that, the addition of surfactants usually provides short-time stability enhancement, while in some research studies, it leads to undesirable effects, like deterioration of heat transfer performance of NFs and viscosity increase [20]. The second step aims to eliminate the negative effect of NPs' initial agglomeration after their addition to the dielectric medium, as they tend to reduce their high surface areas per unit volume [17], [18], [19]. In order to produce uniform colloidal suspensions, each NF sample is subjected to vigorous ultrasonication for 90 min in total, using ultrasonic cleaner Elmasonic S 40 H. The chosen protocol consists of continuous stirring for 30 min, followed by a 15-min break, with the cycle repeated two times. The colloidal stability of each of the samples had been studied in situ both in room and high temperature in previous work of the authors [18], while the representative TEM images of the TiO_2 dispersions in NEO can be found in [21].

In this study, the optimal percentages of TiO_2 and SiC NPs, found in previous studies [18], are examined in terms of aging so as to evaluate the long-term performance of these NFs, which is critical for industrial applications. In higher concentration levels, agglomeration and sedimentation were found, thus excluded from the current study [18]. Lower than 0.004% concentrations in NEO provide mediocre enhancement of the dielectric properties [21].

In Fig. 1, the NF samples are depicted after their production, and their identification is incorporated in Table I.

III. Experimental Part

This section includes the principles under which the measurements (dielectric and thermal) of the NFs under investigation have taken place.

TABLE I
Labeling of the NF Samples

Sample Name (n)	NP Concentration (% w/w)
Base (Matrix)	0
sNF1	NF containing 0.004% SiC
sNF2	NF containing 0.008% SiC
tNF1	NF containing 0.004% TiO_2
tNF2	NF containing 0.008% TiO_2

Fig. 2. Apparatuses used for thermal diffusivity and relative permittivity measurements. (a) NETZSCH LFA 467 Hyper Flash device. (b) Novocontrol Alpha analyzer.

After making the NF samples, the conduction of the thermal and dielectric properties measurements is made using the methods outlined in the following parts of this section. This is required in order to reduce the detrimental impacts of NPs agglomeration/sedimentation, which alters their active concentration in the host liquid and consequently affects their thermal and dielectric performance [18]. According to the findings of our past research [18], TiO_2-based NFs lost stability faster than their SiC equivalents; hence, it is essential to undertake tests within the proper time frame after the homogenization.

The NF samples were left at room temperature in the absence of light, for a month, trying to achieve a natural aging process; thereafter, the same measurements are conducted again to compare the behavior of the samples to that after their synthesis and to link it with the stability research results [18].

A. Conduction of Measurements of Thermal Properties

With respect to the thermal properties, a light on the effect of temperature on the degradation of the thermal diffusivity and conductivity is understudied, wherein the aging effect of 90 °C is reflected primarily on the agglomeration.

So that it is possible to determine the thermal conductivity indirectly, it is first necessary to measure the thermal diffusivity i.e., the speed of heat propagation inside the dielectric. Thermal diffusivity a is measured by utilizing the flash method [13], [17], [22] with the use of NETZSCH LFA 467 apparatus, which is shown in Fig. 2(a). A special liquid cell (LFA test cell, 12.7 mm in diameter) is used to retain the samples. Thermal response is investigated in temperatures

ranging from 25 °C to 85 °C in 10 °C steps, with a maximum temperature of 90 °C. The half-time approach is used to compute thermal diffusivity, which is directly measured from an average of five light pulse shoots [22] according to the following equation:

$$\alpha = \frac{1.38 \cdot L^2}{\pi^2 \cdot t_{1/2}} \tag{3}$$

where a is the thermal diffusivity in mm^2/s, L is the thickness of the sample in mm, and $t_{1/2}$ is the amount of time it takes for the sample's back surface to warm up to 50% of its maximum temperature, in s.

Thermal conductivity is then calculated from Fourier's law of heat conduction as follows [17], [22]:

$$\lambda = \alpha \cdot C_p \cdot \rho \tag{4}$$

where λ is the thermal conductivity in W/(m· K), C_p is the specific heat capacity in J/(g· K) measured by means of differential scanning calorimeter, and ρ is the density of the medium in g/cm^3, which has been equal to the base oil's (0.92 g/cm^3).

B. Conduction of Measurements of Dielectric Properties

With respect to the dielectric performance, in an effort to investigate the dielectric behavior of the understudied NFs, the tand and LI BDV are considered in light of the overall dielectric performance. Tangent delta tests are associated mainly with power losses of NFs under power frequency and they are indicative of their aging (steady-state importance).

The DRS technique is used to calculate the permittivity and tand of the NF samples in the same manner as stated in the preceding section regarding the matrix, after their preparation and after one month of aging. A cylinder-shaped liquid sample holder capacitor is used to hold the NF samples. Afterward, using a Novocontrol Alpha analyzer [Fig. 2(b)], the capacitor sample is supplied with an ac voltage, and the relative permittivity ε_r versus frequency is determined in the range of 1–10^6 Hz at an ambient (25 °C) and at a reasonable elevated temperature of 90 °C. The choice of the elevated temperature corresponds to the necessity to simulate the NFs behavior at upper extreme conditions of the power transformer, where in urgent cases, such as short circuits or high loads under elevated ambient temperatures, the temperature inside the windings can be increased.

The LI BDV experiment under positive polarity concerning the NF and base oil samples at room temperature has been conducted on account of the demands of the IEC 60 897 standard [23]. Impulse tests are associated with the overvoltage behavior of the NF under fast-front overvoltages that may occur in the field, such as lightning-related overvoltages impinging on transformers and transient voltage events. Positive LI BDV is selected as the preferred polarity because most NPs are mainly influenced by the LI BDV under positive polarity, while the negative one remains almost unaffected [24]. On top of this, the mean negative impulse breakdown voltage level is higher than the positive one [25], for the same gap separation distance; therefore, by finding the lightning withstand voltage under positive polarity, the transient performance of the NF under the most unfavorable conditions can be estimated.

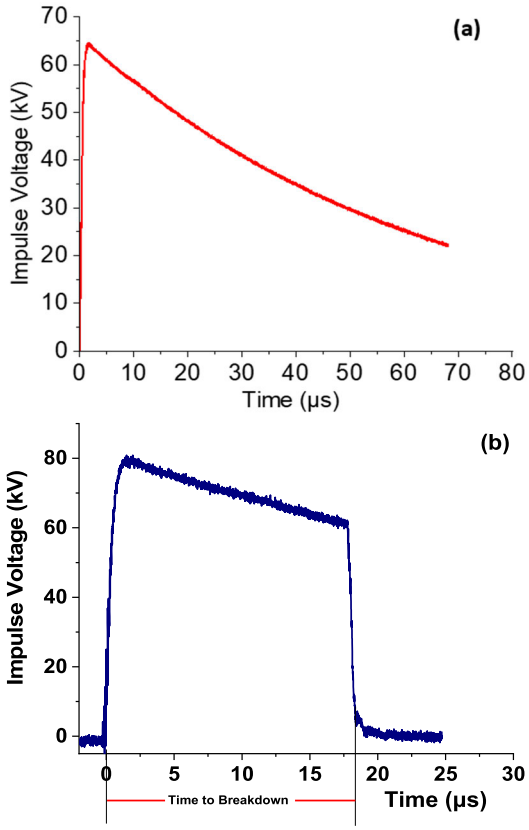

Fig. 3. LIV waveforms. (a) Withstand case (1.2/50 μs). (b) LI breakdown case waveform displaying the breakdown time.

The impulse generator is a two-stage (Marx) Haefely AG device with a maximum output voltage of 400 kV and total energy of 600 J generating LIV 1.2/50 μs. The measurements are carried out in a nonhomogeneous point-sphere field geometry [17]. The point-sphere electrodes in the test cell have a fixed 25-mm spacing. The sphere's diameter is 12.7 mm, while the point has a radius of curvature of 50 μm. The protocol to determine the LI BD performance is the same as that in our previous study [17]. Briefly, three voltage applications occur at the selected levels, beginning from a particular voltage level that is predicted to be lower than the LI BDV. The impulse voltage level is increased if the applied voltage causes no BD [17], until ten breakdowns in total are acquired, and then, the mathematical analysis of the results is performed [1], [3], [6], [17].

The applied LIV is measured through a capacitive voltage divider and monitored through Tektronix DPO4104; 1-GHz, 5-GS/s oscilloscope. A typical LIV signal recorded from the oscilloscope is presented in Fig. 3(a), while a corresponding LI BDV waveform displaying the BD time is depicted in Fig. 3(b).

IV. Results and Discussion

A. Thermal Performance

Fig. 4 shows the average thermal diffusivity values for the samples under investigation obtained from five light pulses

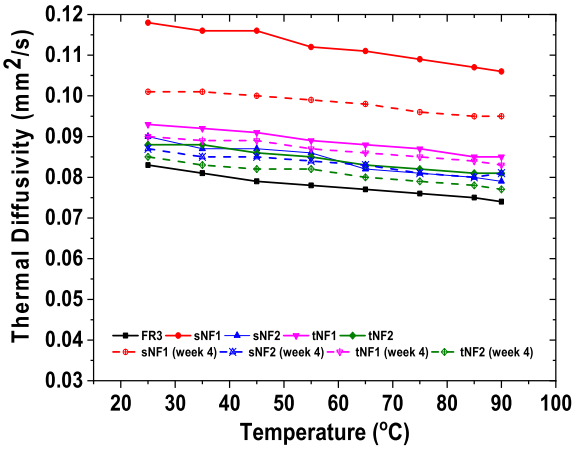

Fig. 4. Thermal diffusivity of as-prepared and one-month aged samples at temperature range from 25 °C to 90 °C.

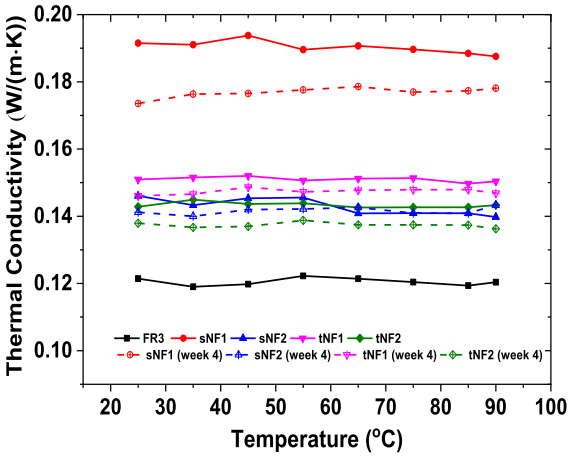

Fig. 5. Thermal conductivity of as-prepared and one-month aged samples at temperature range from 25 °C to 90 °C.

and computed from (3) for the range of the understudied temperature levels. The solid lines represent their response at the time of their synthesis, while the dotted lines demonstrate the repeated measurements after one-month thermal aging regarding the same samples. Fig. 5, on the other hand, displays the mean conductivity values at the same conditions as a function of increasing temperature.

Fig. 4 clearly illustrates how the diffusivity of all NFs has increased in comparison to the matrix oil, with sNF1 showing the most significant enhancement across the entire range of temperature. The same trend is observed in the aged samples as well, albeit their behavior has worsened, probably due to the augmented NPs' tendency to aggregate over time.

sNF1 sample is characterized by enhanced thermal performance, compared to the tNF samples; however, various parameters can still affect this enhancement, including thermal conductivities of the base fluid and the NPs, the volume fraction, the surface area, the shape, and the temperature [26], [27], [28]. Considering the above, the increased thermal conductivity can be attributed to the increased thermal conductivity of the SiC NP with respect to the TiO_2 due to the usage of very low concentrations, with dimensions >10 nm (wherein nanolayers and NP dimensions can highly impact the thermal conductivity) [27]. Despite the numerous micro/nanoscale and macroscale interpretations, explaining and predicting the thermal conductivity behavior of NFs is still a topic of high interest and various theories [27].

On the contrary, the fact that this sample demonstrates better thermal performance than the dispersion with the double concentration means that the NPs' agglomeration in terms of the latter dispersion plays a major role in the thermal conductivity behavior, as it has been reported in other published research articles [29]. While various theories are used for the thermal conductivity of NFs, the agglomeration effect on the thermal conductivity is an extensively challenging topic approached with fractal theories describing the disorder and stochastic process of clustering [30].

Thermally improved performance of NFs used in power transformers is critical since: 1) a system can have increased power for the same size or reduced size for the same power because of the accelerated cooling process with improved dielectric strength and 2) a system can have increased lifetime due to the reduced temperature under normal operating conditions, which also affects the solid insulation (i.e., kraft paper) and transformer itself. There are other numerous applications, combining the thermal and dielectric properties of cooling and insulation systems, such as microelectronics and solid-state lightning, wherein increased thermal properties can tackle the heat dissipation by keeping the same dimensions [31]. The thermal conductivity behavior, as seen in Fig. 5, is similar to the one of thermal diffusivity. sNF1 sample's thermal conductivity is the most enhanced up to 58% with respect to NEO's. It is noteworthy that the largest decrease in thermal properties after aging is observed in sNF1 NF, which has shown the highest increase at the time of its synthesis. It can therefore be concluded that the existence of aggregates, mainly due to aging, affects the thermal properties significantly. As the previous study has already reported [18], the amount of sediments in this NF is negligible; therefore, the entire amount of aggregates is contained in its volume making it hard to dissipate heat.

On the contrary, in the sNF2 NF, the amount of agglomerates has been reduced compared to those present during its composition due to sedimentation, and thus, the reduction in thermal properties is negligible. The same pattern is identified for the two tNF dispersions, where the tNF2 sample, due to the faster aggregation, demonstrates the most significant decrease in the heat dissipation capacity.

B. Relative Permittivity and Loss Tangent

The investigational samples' spectrum changes in dielectric constant at 25 °C and 90 °C are shown in Fig. 6(a) and (b), respectively. The corresponding change of tand is also depicted in Fig. 7(a) and (b), respectively. Fig. 6(a) and (b) indicates that the samples at the lowest NPs' investigated concentrations, shortly after their synthesis, have reduced dielectric constants throughout the entire frequency range, which is mainly related to electrode polarization and interfacial polarization of the Maxwell–Wagner–Sillars type [17].

The following LI BDV results could also be detected in the lowered values of the dielectric constant, which

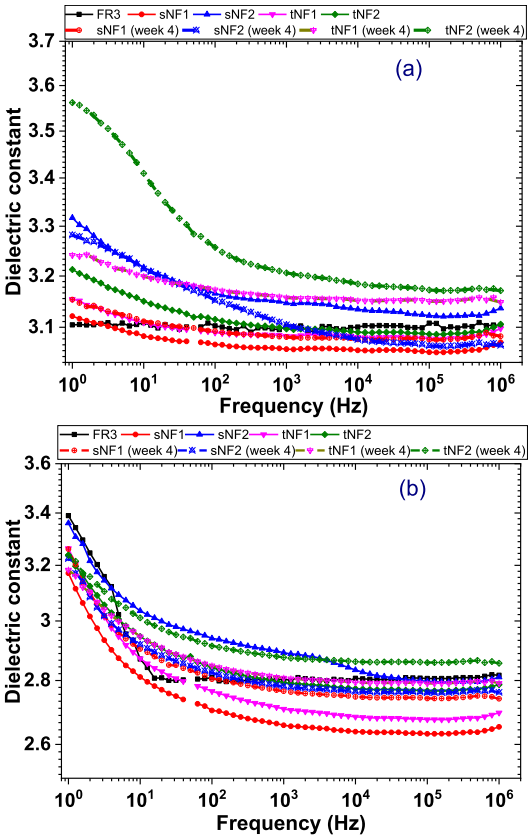

Fig. 6. Variation of dielectric constant versus frequency for the samples freshly prepared and after 4-week aging at (a) 25 °C and (b) 90 °C.

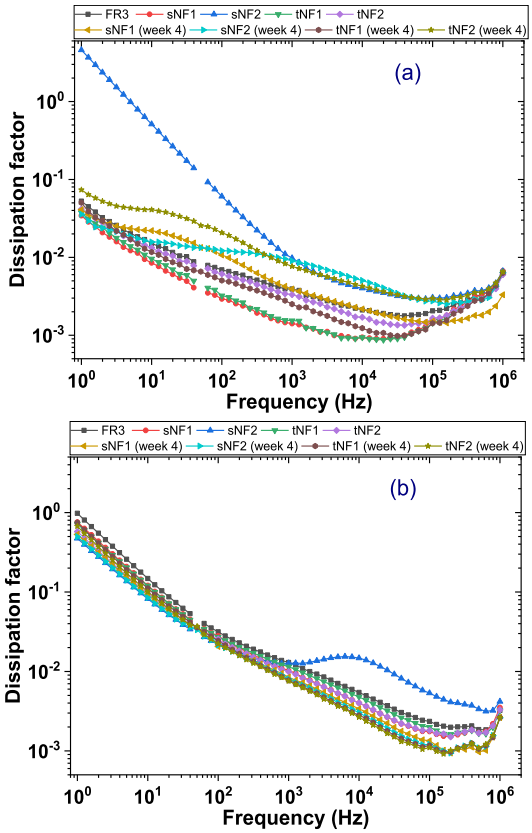

Fig. 7. Variation of dissipation factor versus frequency for the samples freshly prepared and after 4-week aging at (a) 25 °C and (b) 90 °C.

may indicate enhanced dielectric strength of these samples [17], [32]. Additionally, it is clear that all samples included in the study experience a decrease in dielectric constant as temperature rises. The temperature effect might be caused by dipolar orientation polarization processes, which are proportional to 1/T in this frequency range [17]. The NF samples at the highest concentrations on the other hand are characterized by the highest values of dielectric constant at the time of their synthesis, which are lowered after the repetition of the experiment. The influence of NPs' agglomeration/ sedimentation can also be used to explain these findings.

Dynamic light scattering (DLS) results in our previous work [17] have already proven that at these concentrations, rapid aggregation took place; therefore, conductive paths were quickly generated between the electrodes. However, the same samples also presented quick sedimentation, unlike the sNF1 sample, which explains their more similar behavior after one month of aging.

Fig. 7(a) and (b) shows that the tand of the sNF1 and tNF1 samples is lower across the understudied frequencies, with a higher reduction at 25 °C (b). This is a crucial trait because one of the most significant weaknesses of the NEO is the higher tand in relation to MO [5].

Having in mind (2), that has been applied for the estimation of tand, and taking into account that the dielectric constant, ε_r', exhibits weak temperature and frequency dependence (Fig. 6) as compared to tand (logarithmic scale in Fig. 7), it may be concluded that the temperature and frequency dependence of the dielectric losses, ε_r'', rule the observed behavior of tand. Therefore, the increase of tand at 90 °C, the same for all samples, reflects the increase of charge carriers' mobility at the elevated temperature. The existence of these charges may be attributed to impurities in the oil matrix. Similarly, the differences in tand(f) curves shown in Fig. 7(a) reflect the differences in the conductivity and/or the distribution of the NPs within the oil. In this context, the higher tand values of fresh sNF2 sample at 25 °C, especially at low frequencies, point to a particular long range charge mobility process in this sample. In addition, the appearance of a polarization process at the elevated temperature (in the kilohertz frequency region) implies the existence of a particular interfacial polarization due to the inhomogeneous distribution of the SiC NPs. In the aged samples, this particular morphology of the NF has been changed.

C. Lightning Impulse Breakdown Voltage

The mean values and standard deviation of LI BDV and BD time of all the relevant samples are summarized in Tables II and III, respectively. The LI BDV measurements have taken place shortly after synthesizing the NF samples at room temperature, and the outcomes are compared in the next part to the ones of numerical simulation.

The mean breakdown velocity u across the 2.5-cm point-sphere gap is estimated from the following equation [33], [34]:

$$\bar{u} = \frac{d}{t} \tag{5}$$

TABLE II
MEAN VALUE AND STANDARD DEVIATION OF LI BDV EVENTS

Nanofluid Samples	Lightning Impulse Breakdown Voltage	
Sample Label (n)	Mean Value (kV)	Standard Deviation (kV)
Matrix	75.3	2.6
sNF1	82.7	2.4
sNF2	75.4	3.3
tNF1	79.5	2.0
tNF2	76.7	4.0

TABLE III
MEAN VALUE AND STANDARD DEVIATION OF TIME TO BREAKDOWN

Nanofluid Samples	Time to Breakdown	
Sample Label (n)	Mean Value (μs)	Standard Deviation (μs)
Matrix	17.5	1.3
sNF1	19.1	1.1
sNF2	16.8	1.8
tNF1	18.4	1.0
tNF2	17.2	1.2

where d is the gap length (2.5 cm) and t is the average time to BD in μs, as it is shown in Table III. They are calculated as 0.147, 0.136, 0.149, 0.136, and 0.145 cm $\cdot\, \mu s^{-1}$ for matrix, sNF1, sNF2, tNF1, and tNF2, respectively, which correlate to slow streamer propagation to faster modes regarding the sNF1 and tNF1 samples [33], [34].

The obtained LI BDV results can be explained by the theory, according to which NPs operate as shallow traps for charge carriers [11], [17], [18]. When an electric field above a critical threshold is applied, due to the fact that ε_r' of the integrated NPs and the matrix vary significantly, according to DRS results [17], polarized charges (due to their semiconductive nature of both kinds of NPs) are produced at the oil–NP interface and inhibit streamer growth. Consequently, fast electrons could be trapped in shallow traps; as a result, higher external electric field values need to be applied to enable the charge carriers to be released and traverse the gap.

However, doubling the NPs' loading concerning both sNF and tNF samples reduces the LI BDV. The Derjaguin–Landau–Verwey–Overbeek (DLVO) theory's expression of colloidal stability [2], [3], [18] can be used to explain the dissimilar LI BDV behavior of the sNF2 and tNF2 samples. According to this, electrostatic repulsion and van der Waals attraction forces that emerge from the electrical double layers (EDLs) formed around each charged NP combine to form the overall interaction between two NPs. When the interparticle distance decreases, which occurs with larger NP concentrations, the intensity of van der Waals attraction energy correspondingly

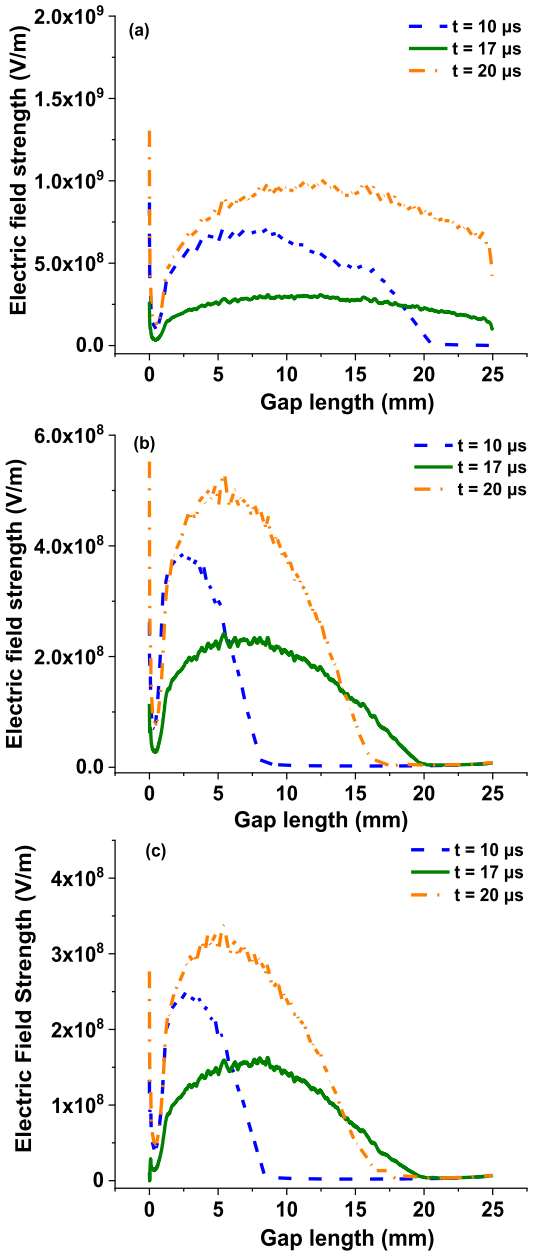

Fig. 8. Distribution of electric field strength versus the gap length at the specified time intervals for (a) base, (b) sNF1, and (c) sNF2.

increases. This observation clarifies the presence of a threshold level—the ideal concentration in terms of LI BDV maximization—that has been recorded in several earlier investigations [2], [3], [4], [8], [18].

V. NUMERICAL MODEL RESULTS

To confirm how the NPs' agglomeration affects the dielectric performance of synthesized NFs, the numerical model developed in COMSOL Multiphysics and analytically described in our previous study [17] is used to simulate the dielectric behavior of matrix, sNF1, and sNF2, when exposed to LIV 80 kV, 1.2/50 μs.

The simulation time has lasted 20 μs and includes a 50-ns time step [17]. As referred in [17], the NPs' charging process depends on the highest possible trapped charge density

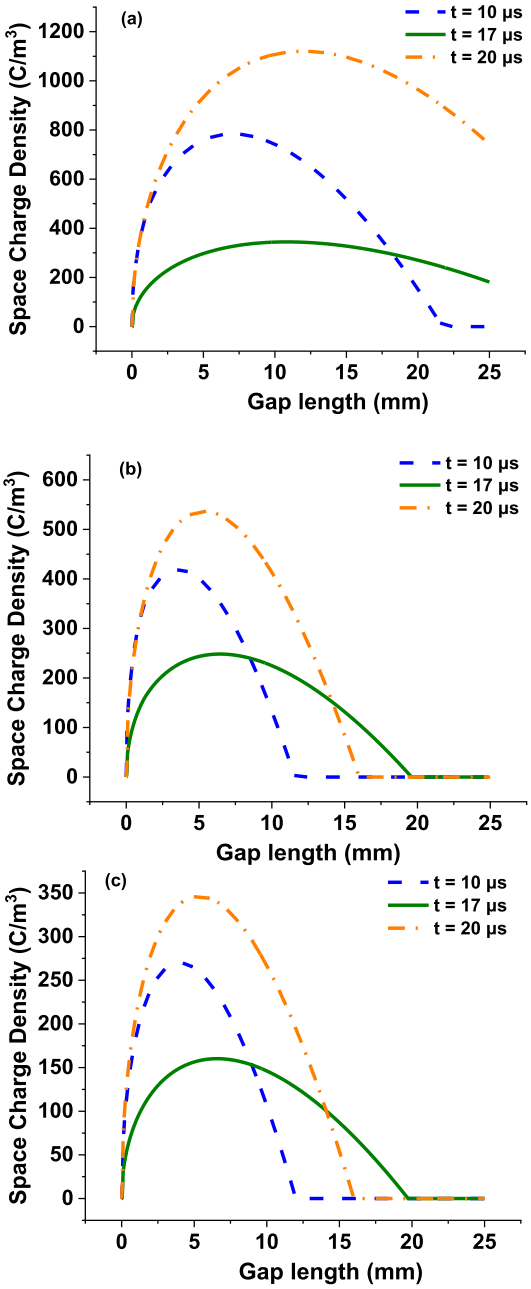

Fig. 9. Distribution of space charge density versus the gap length at the specified time intervals for (a) base, (b) sNF1, and (c) sNF2.

$\rho_{\text{np,sat}} = n_{\text{np}} \cdot Q_s$, where n_{np} is the NPs' number density and Q_s expresses the highest amount of charge captured by each NP. Considering that the NPs in both NF samples are uniformly dispersed, the saturation charge density in sNF1 and sNF2 is computed as -359 and -718 C/m^3, respectively.

The point electrode has been subjected to a positive LIV 80 kV, 1.2/50 μs, and the electric field strength along with the space charge density is computed across the 25-mm gap at specific time intervals, namely, at 10, 17, and 20 μs. Fig. 8(a)–(c) presents the distribution of the electric field strength across the gap, while Fig. 9(a)–(c) depicts the space charge densities versus the gap length for the matrix, sNF1, and sNF2, respectively.

Figs. 8 and 9 demonstrate that the simulated and experimental results are very similar as regard to the Base and sNF1 samples. It is evident that in the case of Base, an 80-kV LIV is adequate to span the gap, in contrast to the sNF1. The anticipated LI BDV of sNF2 should, however, be larger than that of sNF1 since the electric field strength and space charge density are even lower in terms of sNF2, a fact that would mean that the expected experimental LI BDV of this NF should be higher. In this circumstance, the simulated findings and the experimental results mismatch. Probably due to the NPs' quick aggregation regarding this dispersion, the real saturation charge density is not the one taken into account for simulation purposes, as it has already been proven regarding this dispersion through DLS measurements [18].

VI. Conclusion

This study compares the effect of aging of NFs based on TiO_2 and SiC NPs (two weight percentage ratios) on the thermal and dielectric properties. The conclusion of this work are summarized as follows.

The NF sample containing the lowest amount of SiC NPs possesses the highest thermal diffusivity and conductivity maximization, while its dielectric constant is the most reduced when compared to the values of the matrix oil.

1) After one month of aging, the low concentration NF's properties are worsened but still remain the most enhanced, probably due to the existence of agglomerates without sediments.
2) Comparing the LI BDV results to simulation results proved that the adopted numerical model could successfully predict that an 80-kV LIV level is enough to cause breakdown for the case of Base while sNF1 sample withstands this stress. On the other hand, the NF containing double concentration shows lower dielectric strength experimentally, probably attributing this behavior to NPs' agglomeration regarding this dispersion, which is neglected in numerical modeling.

As part of future works, it would be of major interest to study the influence of aging in physicochemical properties, such as acidity and interfacial tension, which are also very important for the selection of a NF sample as replacement of the current used transformer oil.

Acknowledgment

The authors would like to acknowledge Dr. Aspasia Antonelou from the Foundation for Research and Technology Hellas, Patras, Greece for the preparation of the NF samples, and Aimilia Barmpaki from the Condensed Matter Division, Department of Physics, University of Patras, for the conduction of DRS measurements of the NPs. Moreover, they want to thank Kevin Rapp, Principal Scientist at Cargill Bioindustrial, for the natural ester supply (FR3).

References

[1] U. Khaled and A. Beroual, "AC dielectric strength of synthetic ester-based Fe_3O_4, Al_2O_3 and SiO_2 nanofluids—Conformity with normal and Weibull distributions," *IEEE Trans. Dielectr. Electr. Insul.*, vol. 26, no. 2, pp. 625–633, Apr. 2019.

[2] E. G. Atiya, D. A. Mansour, R. M. Khattab, and A. M. Azmy, "Dispersion behavior and breakdown strength of transformer oil filled with TiO_2 nanoparticles," *IEEE Trans. Dielectr. Electr. Insul.*, vol. 22, no. 5, pp. 2463–2472, Oct. 2015.

[3] M. Rafiq, M. Shafique, A. Azam, and M. Ateeq, "Transformer oil-based nanofluid: The application of nanomaterials on thermal, electrical and physicochemical properties of liquid insulation—A review," *Ain Shams Eng. J.*, vol. 12, no. 1, pp. 555–576, Mar. 2021.

[4] H. Cong, H. Shao, Y. Du, X. Hu, W. Zhao, and Q. Li, "Influence of nanoparticles on long-term thermal stability of vegetable insulating oil," *IEEE Trans. Dielectr. Electr. Insul.*, vol. 29, no. 5, pp. 1642–1650, Oct. 2022.

[5] A. Beroual and U. Khaled, "Statistical investigation of lightning impulse breakdown voltage of natural and synthetic ester oils-based Fe_3O_4, Al_2O_3 and SiO_2 nanofluids," *IEEE Access*, vol. 8, pp. 112615–112623, 2020.

[6] J. Jacob, P. Preetha, and T. K. Sindhu, "Stability analysis and characterization of natural ester nanofluids for transformers," *IEEE Trans. Dielectr. Electr. Insul.*, vol. 27, no. 5, pp. 1715–1723, Oct. 2020.

[7] P. Thomas, N. E. Hudedmani, R. T. A. R. Prasath, N. K. Roy, and S. N. Mahato, "Synthetic ester oil based high permittivity $CaCu_3Ti_4O_{12}$ (CCTO) nanofluids an alternative insulating medium for power transformer," *IEEE Trans. Dielectr. Electr. Insul.*, vol. 26, no. 1, pp. 314–321, Feb. 2019.

[8] Y. Zhong et al., "Insulating properties and charge characteristics of natural ester fluid modified by TiO_2 semiconductive nanoparticles," *IEEE Trans. Dielectr. Electr. Insul.*, vol. 20, no. 1, pp. 135–140, Feb. 2013.

[9] M. Fasehullah, F. Wang, and S. Jamil, "Significantly elevated AC dielectric strength of synthetic ester oil-based nanofluids by varying morphology of CdS nano-additives," *J. Mol. Liquids*, vol. 353, May 2022, Art. no. 118817.

[10] H. Khelifa, E. Vagnon, and A. Beroual, "AC breakdown voltage and partial discharge activity in synthetic ester-based fullerene and graphene nanofluids," *IEEE Access*, vol. 10, pp. 5620–5634, 2022.

[11] W. Sima, J. Shi, Q. Yang, S. Huang, and X. Cao, "Effects of conductivity and permittivity of nanoparticle on transformer oil insulation performance: Experiment and theory," *IEEE Trans. Dielectr. Electr. Insul.*, vol. 22, no. 1, pp. 380–390, Feb. 2015.

[12] A. A. Adekunle, S. O. Oparanti, and I. Fofana, "Performance assessment of cellulose paper impregnated in nanofluid for power transformer insulation application: A review," *Energies*, vol. 16, no. 4, 2023, Art. no. 2002.

[13] K. Koutras, S. Tegopoulos, G. Peppas, I. Gonos, A. Kyritsis, and E. Pyrgioti, "Influence of SiC and TiO_2 nanoparticles on the dielectric and thermal properties of natural ester based nanofluids," in *Proc. IEEE 21st Int. Conf. Dielectr. Liquids (ICDL)*, May 2022, pp. 1–4.

[14] K. S. Suganthi and K. S. Rajan, "Metal oxide nanofluids: Review of formulation, thermo-physical properties, mechanisms, and heat transfer performance," *Renew. Sustain. Energy Rev.*, vol. 76, pp. 226–255, Sep. 2017.

[15] A. J. Amalanathan, N. Harid, H. Griffiths, and R. Sarathi, "Impact of adding activated bentonite to thermally aged ester-based TiO_2 nanofluids on insulation performance," *IET Nanodielectr.*, vol. 4, no. 2, pp. 63–74, Jun. 2021.

[16] F. Ahmad, A. A. Khan, Q. Khan, and M. R. Hussain, "State-of-art in nano-based dielectric oil: A review," *IEEE Access*, vol. 7, pp. 13396–13410, 2019.

[17] K. N. Koutras et al., "Dielectric and thermal response of TiO_2 and SiC natural ester based nanofluids for use in power transformers," *IEEE Access*, vol. 10, pp. 79222–79236, 2022.

[18] K. N. Koutras, A. E. Antonelou, I. A. Naxakis, V. P. Charalampakos, E. C. Pyrgioti, and S. N. Yannopoulos, "In-situ high temperature study of the long-term stability and dielectric properties of nanofluids based on TiO_2 and SiC dispersions in natural ester oil at various concentrations," *J. Mol. Liquids*, vol. 359, Aug. 2022, Art. no. 119284.

[19] G. D. Peppas et al., "Ultrastable natural ester-based nanofluids for high voltage insulation applications," *ACS Appl. Mater. Interfaces*, vol. 8, no. 38, pp. 25202–25209, Sep. 2016.

[20] B. X. Du, X. L. Li, and M. Xiao, "High thermal conductivity transformer oil filled with BN nanoparticles," *IEEE Trans. Dielectr. Electr. Insul.*, vol. 22, no. 2, pp. 851–858, Apr. 2015.

[21] K. N. Koutras, I. A. Naxakis, A. E. Antonelou, V. P. Charalampakos, E. C. Pyrgioti, and S. N. Yannopoulos, "Dielectric strength and stability of natural ester oil based TiO_2 nanofluids," *J. Mol. Liquids*, vol. 316, Oct. 2020, Art. no. 113901.

[22] P. A. Klonos et al., "Effects of CNTs on thermal transitions, thermal diffusivity and electrical conductivity in nanocomposites: Comparison between an amorphous and a semicrystalline polymer matrix," *Soft Matter*, vol. 15, pp. 1813–1824, Jan. 2019.

[23] *Methods for the Determination of the Lightning Impulse Breakdown Voltage of Insulating Liquids*, IEC Standard 60897, 1987.

[24] Y. Lv et al., "Effect of TiO_2 nanoparticles on streamer propagation in transformer oil under lightning impulse voltage," *IEEE Trans. Dielectr. Electr. Insul.*, vol. 23, no. 4, pp. 2110–2115, Aug. 2016.

[25] V. A. Primo, B. García, J. C. Burgos, and D. Pérez-Rosa, "Investigation of the lightning impulse breakdown voltage of mineral oil based Fe_3O_4 nanofluids," *Coatings*, vol. 9, no. 12, 2019, Art. no. 799.

[26] X. Li, C. Zou, L. Zhou, and A. Qi, "Experimental study on the thermo-physical properties of diathermic oil based SiC nanofluids for high temperature applications," *Int. J. Heat Mass Transf.*, vol. 97, pp. 631–637, Jun. 2016.

[27] X. Q. Wang and A. S. Mujumdar, "Heat transfer characteristics of nanofluids: A review," *Int. J. Thermal Sci.*, vol. 46, no. 1, pp. 1–19, 2007.

[28] Z. Said, R. Saidur, A. Hepbasli, and R. A. Rahim, "New thermophysical properties of water based TiO_2 nanofluid—The hysteresis phenomenon revisited," *Int. Commun. Heat Mass Transf.*, vol. 58, pp. 85–95, Nov. 2014.

[29] I. Chopkar, S. Sudarshan, P. K. Das, and I. Manna, "Effect of particle size on thermal conductivity of nanofluid," *Metal. Mater. Trans. A*, vol. 39, pp. 1535–1542, Feb. 2008.

[30] B.-X. Wang, L.-P. Zhou, and X.-F. Peng, "A fractal model for predicting the effective thermal conductivity of liquid with suspension of nanoparticles," *Int. J. Heat Mass Transf.*, vol. 46, no. 14, pp. 2665–2672, 2003.

[31] P. Keblinski, J. A. Eastman, and D. G. Cahill, "Nanofluids for thermal transport," *Mater. Today*, vol. 8, no. 6, pp. 36–44, 2005.

[32] D. A. Mansour, A. M. Elsaeed, and M. A. Izzularab, "The role of interfacial zone in dielectric properties of transformer oil-based nanofluids," *IEEE Trans. Dielectr. Electr. Insul.*, vol. 23, no. 6, pp. 3364–3372, Dec. 2016.

[33] O. Lesaint and G. Massala, "Positive streamer propagation in large oil gaps: Experimental characterization of propagation modes," *IEEE Trans. Dielectr. Electr. Insul.*, vol. 5, no. 3, pp. 360–370, Jun. 1998.

[34] Q. Liu and Z. D. Wang, "Streamer characteristic and breakdown in synthetic and natural ester transformer liquids under standard lightning impulse voltage," *IEEE Trans. Dielectr. Electr. Insul.*, vol. 18, no. 1, pp. 285–294, Feb. 2011.

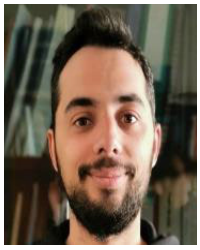

Konstantinos N. Koutras was born in Korinthos, Greece, in 1992. He received the integrated master's degree in electrical and computer engineering and the M.Sc. degree in green electric power from the Department of Electrical and Computer Engineering, University of Patras, Patras, Greece, in 2016 and 2018, respectively, where he is currently pursuing the Ph.D. degree in insulating nanofluids.

Georgios D. Peppas (Senior Member, IEEE) was born in Rustenburg South Africa, in 1987. He received the Diploma degree in electrical engineering and the Ph.D. degree from the Department of Electrical and Computer Engineering, University of Patras, Patras, Greece, in 2011 and 2016, respectively.

He has been a Research and Development Manager of Raycap leading innovation in surge protective devices and a Technical Manager of the High Current Laboratory of Raycap, Drama, Greece, since 2016. His research interests include lightning and surge protection and nanofluids for high-voltage applications.

Sokratis N. Tegopoulos was born in Athens, Greece, in 1977. He received the B.Sc. degree in natural sciences from Hellenic Open University, Patra, Greece, in 2016, and the M.Sc. degree in applied physics from the School of Applied Mathematical and Physical Sciences, National Technical University of Athens (NTUA), Athens, Greece, in 2018, where he is currently pursuing the Ph.D. degree.

His research interests include the study of structure–properties relationship in (bio)polymer nanocomposite materials and hydration properties of several materials.

Apostolos Kyritsis was born in Berlin, Germany, in 1966. He received the Diploma degree in physics and the Ph.D. degree in materials science-physics from the University of Athens, Greece, in 1988 and 1995, respectively.

His scientific interests include dielectric, thermal and vapor sorption studies in ionic crystals, ceramics, polymers and complex polymeric systems and structure–property relationships in polymers, biopolymers, nanocomposites, and hydration properties of inorganic and organic materials.

Andreas G. Yiotis was born in Athens, Greece, in 1974. He received the Diploma degree in chemical engineering and the Ph.D. degree in transport phenomena in porous media from the School of Chemical Engineering, National Technical University of Athens (NTUA), Athens, Greece, 1997 and 2003, respectively.

He is currently an Assistant Professor in fluid mechanics and petroleum engineering with the School of Mineral Resources Engineering, Technical University of Crete, Chania, Greece.

Thomas E. Tsovilis (Senior Member, IEEE) was born in Piraeus, Greece, in 1983. He received the M.Eng. and Ph.D. degrees in electrical and computer engineering from the Aristotle University of Thessaloniki (AUTh), Thessaloniki, Greece, in 2005 and 2010, respectively.

He was the Director of the High Current Laboratories, Raycap, Greece and Slovenia (2012–2018). In 2018, he joined AUTh, where he is currently an Assistant Professor. His research interests include the broad area of high-voltage engineering with emphasis given to electrical discharges, lightning protection, and insulation coordination for power systems.

Ioannis F. Gonos (Senior Member, IEEE) was born in Artemisio, Arcadia, Greece, in 1970. He received the Diploma degree in electrical engineering and the Ph.D. degree from the National Technical University of Athens (NTUA), Athens, Greece, in 1993 and 2002, respectively.

He is currently an Associate Professor with the NTUA. His research interests include concern grounding systems, dielectric liquids, high voltages, measurements, and insulators.

Eleftheria C. Pyrgioti (Member, IEEE) was born in Kanalia, Karditsa, Greece, in 1958. She received the Diploma degree in electrical engineering and the Ph.D. degree from the Department of Electrical and Computer Engineering, University of Patras, Patras, Greece, in 1981 and 1991, respectively.

She is currently a Professor with the Department of Electrical and Computer Engineering, University of Patras. Her research interests include concern high-voltage systems, lightning protection, high-voltage insulation, dielectric liquids, distributed generation, and renewable energy.